

Reactions and Phase Transformation in SiO_2 – ZrO_2 Sol–Gel Coated Alumina Powder

Stefan Ebener* & Wolfgang Winter†

Institute of Mineralogy, Technical University of Darmstadt, Schnittspahnstraße 9, D-64287 Darmstadt, Germany

(Received 20 December 1994; revised version received 18 January 1996; accepted 20 February 1996)

Abstract

TEOS and zirconium-*n*-propoxide have been hydrolysed in a two-step process in the presence of Al_2O_3 powder in order to coat the alumina grains with two layers of SiO_2 and ZrO_2 . The reactions and phase transformations during sintering of the coated powders to a mullite–zirconia composite were investigated by means of differential thermal analyses, X-ray diffraction, transmission electron microscopy and scanning electron microscopy. The sequence of coating influences the crystallization temperature of tetragonal zirconia from the amorphous ZrO_2 layer. In the Al_2O_3 powder that was coated first with ZrO_2 the temperature of the tetragonal zirconia crystallization is 65 K lower than in the powder coated first with SiO_2 . Mullite is not formed through the direct reaction of Al_2O_3 cores and the amorphous SiO_2 layer, but only through the reaction of Al_2O_3 with the metastable precursor phases cristobalite and zircon (ZrSiO_4). A second generation of tetragonal zirconia crystals is formed during the decomposition of zircon, simultaneously increasing the tetragonal to monoclinic ZrO_2 ratio. Copyright © 1996 Elsevier Science Ltd

Deux couches, une d'oxyde de zirconium et l'autre d'oxyde de silicium, ont été appliquées sur les grains d'une poudre fine d'alumine en hydrolysant successivement, du TEOS et du *n*-propoxide de zirconium. Les réactions et transformations des phases lors du frittage des grains enrobés afin d'obtenir un composite mullite–zircone ont été étudiées par DTA, XRD, TEM et MEB. L'ordre dans lequel les couches sont déposées influence la température de cristallization de la phase tétragonale de l'oxyde de zirconium à partir de la couche amorphe de ZrO_2 . Lorsque la poudre de Al_2O_3 est d'abord recouverte d'une couche de ZrO_2 , la température de cristalliza-

tion de l'oxyde de zirconium tétragonal est plus basse (de 65K) que si la poudre est enduite en premier d'une couche de SiO_2 . Dans les deux cas, la mullite n'est jamais formée par réaction directe entre l'alumine et la couche amorphe de SiO_2 , mais seulement par réaction de Al_2O_3 avec des phases intermédiaires métastables, cristobalite et zircon (ZrSiO_4). De l'oxyde de zirconium tétragonal se forme également par la réaction secondaire de décomposition du zircon, augmentant ainsi la proportion entre les phases tétragonale et monoclinique de ZrO_2 .

In einem zweistufigen Prozeß wurden durch Hydrolyse von TEOS und Zirkon-*n*-Propoxid zwei Schichten, bestehend aus ZrO_2 und SiO_2 , auf die Körner eines Al_2O_3 -Pulvers abgeschieden. Die Reaktionen und Phasenumwandlungen während der Sinterung der beschichteten Pulver zu einer Mullit–Zirkonoxid Dispersionskeramik wurden mittels DTA, XRD, TEM und REM untersucht. Die Reihenfolge der Beschichtungen beeinflusst die Kristallisationstemperatur von tetragonalem Zirkonoxid in der amorphen ZrO_2 -Schicht. So zeigt das Al_2O_3 Pulver, bei dem zuerst die ZrO_2 -Schicht abgeschieden wurde, eine um 65 K niedriger einsetzende Kristallisation von tetragonalem ZrO_2 als das Pulver, das zuerst mit einer SiO_2 -Schicht beschichtet wurde. Mullit wird nicht durch eine direkte Reaktion der Al_2O_3 -Kerne mit der amorphen SiO_2 -Schicht gebildet, sondern entsteht durch Reaktion des Al_2O_3 mit den metastabilen Vorläuferphasen Cristobalit und Zirkon (ZrSiO_4). Eine zweite Generation von tetragonalen ZrO_2 Kristalliten wird durch den Zerfall des Zirkons gebildet, wodurch sich gleichzeitig das Verhältnis von tetragonalem zu monoklinem ZrO_2 erhöht.

1 Introduction

The properties of advanced ceramics such as homogeneity, density and microstructure are strongly

*Present address: ITC-WGT/TM, Forschungszentrum Karlsruhe, Postfach 3640, D-76021 Karlsruhe, Germany.

†Present address: Laboratoire de Science des Matériaux Vitreux, Université Montpellier II, F-34095 Montpellier, France.

dependent on the characteristics of the starting powders. Some powder characteristics such as sintering behaviour or reactivity depend mainly on the properties of the surface. Other powder surface-related properties that are of interest for diverse applications such as pigments, magnetic tapes, pharmaceuticals, catalysts and dispersion-strengthened alloys include surface charge, as well as magnetic, optical and adsorptive characteristics. Hence, in recent years several new powder synthesis techniques have been developed, one of them being the hydrolysis and condensation of metal alkoxides or salts via the sol-gel technique. Work has been done to control the powder surface properties by coating particles via the sol-gel technique with a thin layer of different chemical composition. An extensive review of the coating technique is given by Sparks¹ and Garg and Matijevic.²

Major areas for the use of coated powders are the improvement of sinterability and the homogeneous incorporation of additives. For example, the difficulties in sintering electroceramic materials such as ferrites, PMZN relaxor dielectrics, doped SnO_2 or BaTiO_3 can be overcome by coating the powders with a layer consisting of amorphous SiO_2 together with Li_2O or B_2O_3 .³⁻⁵ The densification of such powders proceeds via a liquid-phase sintering mechanism which allows the sintering temperatures and the total amount of incorporated second phases to be lowered compared with the conventional mixing method. The coating technique also helped in the homogeneous incorporation of dopants, counterdopants and additives into PTCR BaTiO_3 thermistors. Numerous studies exist in the literature concerning the kinetics of viscous sintering of glass powders with rigid inclusions and coated inclusion particles.⁶⁻¹⁰

Another important field for the application of coated powders is the formation of particulate- or whisker-reinforced materials. Homogeneous composites with sufficient densities can be obtained by sintering Si_3N_4 powder coated with Al_2O_3 and/or Y_2O_3 , or by sintering SiC whiskers coated with Al_2O_3 .¹¹⁻¹⁵ Zirconia-toughened alumina, mullite, spinel and cordierite ceramics were also formed from coated starting powders.¹⁶⁻¹⁹ In the case of cordierite composites, the ZrO_2 coating also yields an evident improvement of the powder sinterability.

Sacks *et al.*^{20,21} developed a process for the fabrication of mullite ceramics and mullite-zirconia/alumina or mullite-SiC composites referred to as transient viscous sintering (TVS). This method starts from alumina, ZrO_2 and SiC particles that have been coated with an amorphous SiO_2 layer. These particles could be sintered to almost full

density at about 1300°C via viscous flow of the amorphous coating and then converted to mullite through the reaction of SiO_2 and the Al_2O_3 cores at 1500–1600°C. A combination of sintering and reaction between inner cores and outer coatings was also used to fabricate aluminium titanate ceramics from TiO_2 -coated alumina particles.²²

In our study alumina particles were coated with a double layer consisting of SiO_2 and ZrO_2 . Sintering of these powders at 1500–1550°C yields dense mullite-zirconia composites.²³ This paper reports the phase formation and the reactions during heating between the alumina cores and the two coatings. Furthermore, the effects of the sequence of the SiO_2 and ZrO_2 coatings on these reactions were investigated.

2 Experimental Procedure

The coatings of silica and zirconia on alumina particles were achieved by controlled hydrolysis of tetraethylorthosilicate (TEOS) and zirconium-n-propoxide (Alpha Products) in an alcoholic dispersion of fine-grained alumina powder. For the synthesis, a fraction of Al_2O_3 powder, with a grain size not exceeding 1 μm and an average grain size of 0.35 μm , was used, which had been separated by centrifuge from a commercial α -alumina powder (Martoxid CS400/M). The hydrolysis of the two metal organic components was carried out separately in a two-step process, where anhydrous 2-propanol was used as reaction medium for the hydrolysis of zirconium-n-propoxide and ethanol for the hydrolysis of TEOS. The molar ratio of Al_2O_3 to TEOS was 3:2, while zirconium-n-propoxide was added corresponding to 20 wt% of zirconia in the final product. For each sample 6 g of alumina powder was used, yielding about 10 g of coated powder. The total volume of alcohol in each hydrolysis step added up to 500 cm.³

For the coating process, the alumina powder or single-coated powder was dispersed ultrasonically in the required alcohol and the precursor was then added while intensively stirring. The suspension was heated under reflux to a temperature of 50°C for 2 h. TEOS was hydrolysed by adding a mixture of ammoniated water in ethanol ($R_{\text{NH}_3} = 2$, $R_{\text{H}_2\text{O}} = 4$), whereas for the hydrolysis of zirconium-n-propoxide a mixture of distilled water in 2-propanol was used ($R_{\text{H}_2\text{O}} = 15$). Two powders have been synthesized which differ in the sequence of the alkoxide addition: in powder ZT zirconium-n-propoxide was hydrolysed first and TEOS hydrolysed in a second step; in powder TZ the sequence was reversed. After each hydrolysis step

the powders were separated from the reaction medium with a centrifuge, washed with ammoniated water and dried at 100°C.

The coated powders were characterized using transmission electron microscopy (TEM) equipped with a device for energy-dispersive X-ray analysis (EDX) (Philips CM12, 120 kV). The powder samples for the TEM studies were dispersed ultrasonically in ethanol and applied on Formvar-coated Cu nets. The grain size distribution of the powders was measured by means of X-ray sedimentation methods (Sedigraph 5000D). The powders were studied also by means of differential thermal analysis (DTA) (Netzsch 404EP, heating rate 7.5 K min⁻¹).

For further studies, pellets of 5 mm in diameter and 5 mm in height were formed by uniaxial pressing. These samples were isothermally annealed for 4 to 12 h at temperatures ranging from 900 to 1550°C. Crystallization and reactions between

phases as a function of temperature were monitored by X-ray powder diffraction (XRD) methods. The microstructures were studied by means of scanning electron microscopy (SEM) (Philips SEM505).

3 Results

Figures 1 and 2 show the result of the coating process on the alumina powder. The individual SiO₂ and ZrO₂ coatings are difficult to distinguish because they superimpose each other with the exception of the very rim. On Fig. 2 the inner ZrO₂ coating and the outer SiO₂ coating are marked with arrows. In both cases, samples ZT and TZ, concentration profiles of Al₂O₃, ZrO₂ and SiO₂ were measured by means of EDX in the nanoprobe mode. Due to superposition of the coatings with Al₂O₃ the EDX data have merely a

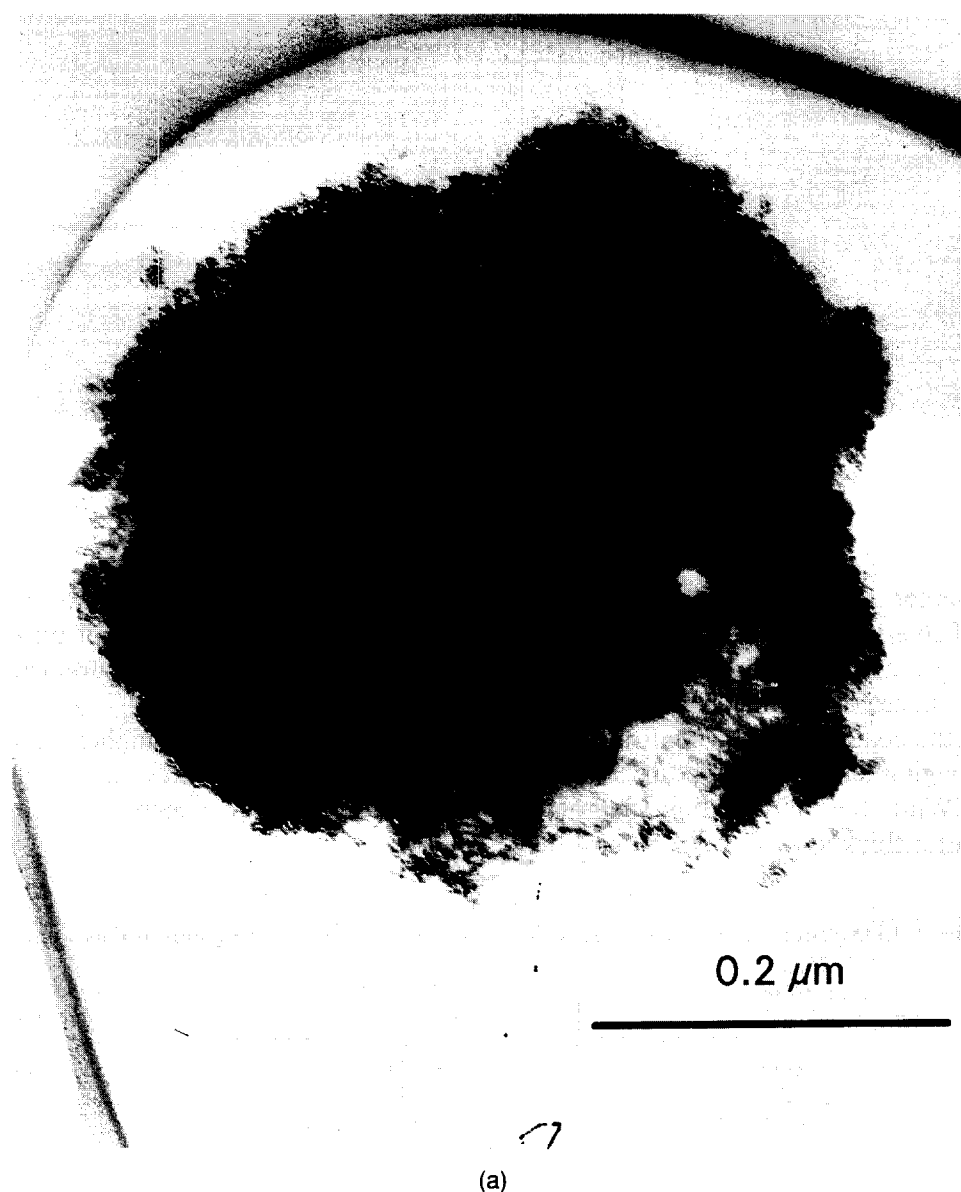
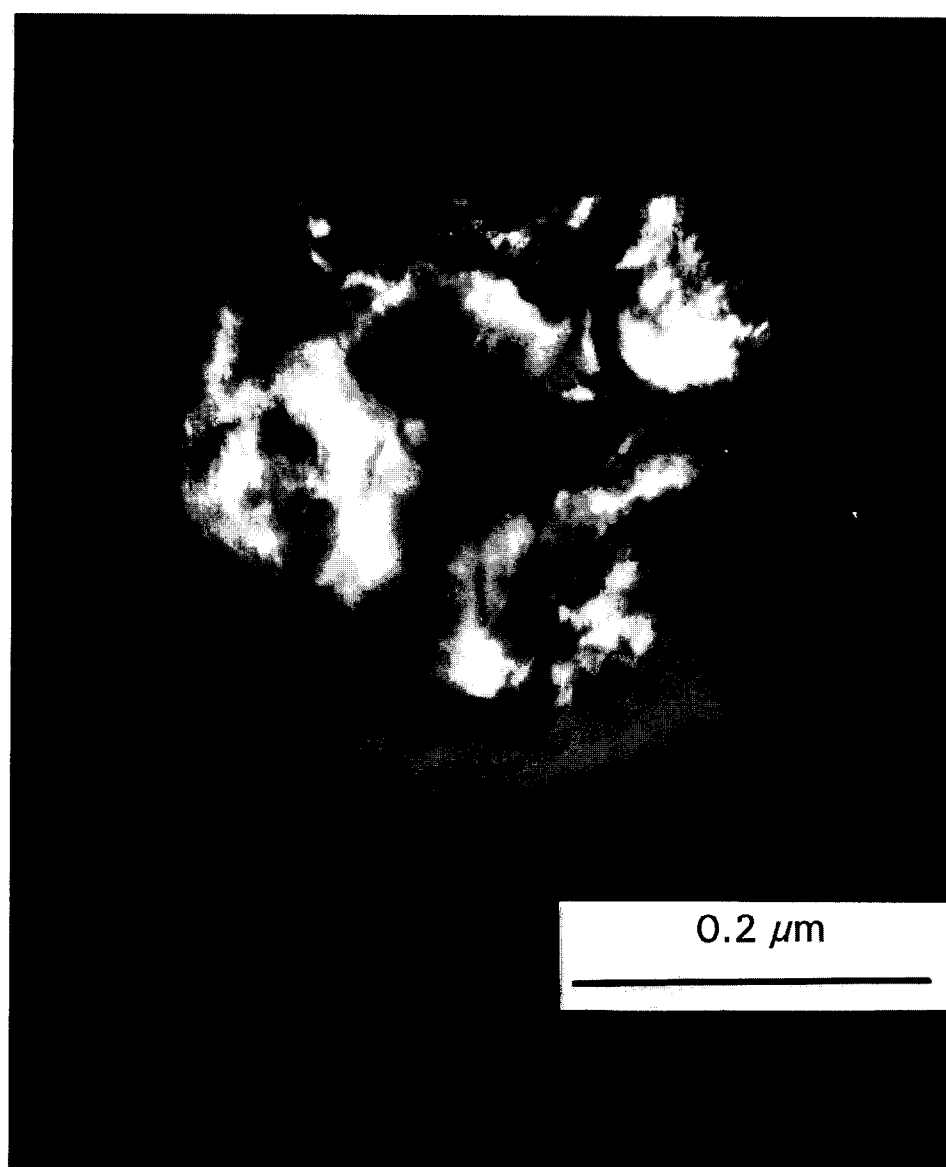


Fig. 1. TEM micrographs of powder TZ after coating with SiO₂ and ZrO₂: (a) bright-field and (b) dark-field image with 10-1 of Al₂O₃.



(b)

Fig. 1.—Contd.

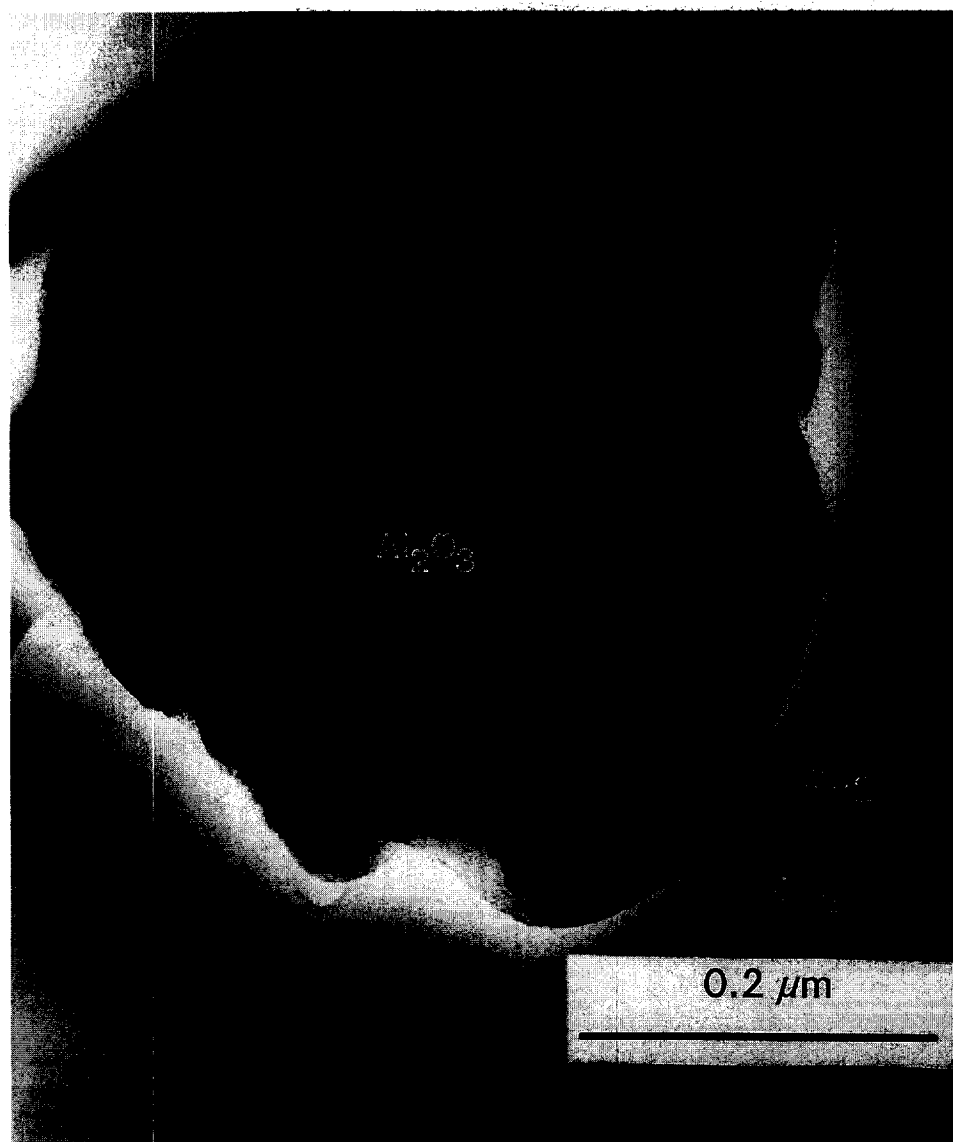
qualitative character. However, comparing the EDX results in Table 1 of the measurements taken from the coated grains shown in Figs 1 and 2, as well as from their mixed layers, the expected respective sequence of the coatings can be confirmed.

Diffraction imaging showed that both coatings are amorphous. While the SiO_2 coating is smooth and compact with a thickness of about 50 nm, the

ZrO_2 coating has a coarser and more fluffy structure resulting in a thickness of up to 100 nm. The Sedigraph grain size measurements gave mean particle sizes of 2.5 and 2.7 μm for TZ and ZT, respectively, which are higher than the expected ones. This is mainly due to an agglomeration of the coated powder, which was also observed with TEM.

Table 1. EDX results as measured in TEM in the nanoprobe mode of the grains in Figs 1 and 2

Sample	Oxide	EDX measurement over the whole grain	EDX measurement in the middle of the coating
TZ	Al_2O_3	45.0	6.3
	SiO_2	24.8	35.1
	ZrO_2	30.2	58.6
ZT	Al_2O_3	48.4	15.0
	SiO_2	27.1	45.2
	ZrO_2	24.5	39.8



(a)

Fig. 2. TEM micrographs of powder ZT after coating with ZrO₂ and SiO₂. The layers of ZrO₂ and SiO₂ are marked at the very rim of the particle. (a) Bright-field and (b) dark-field image with 10-1 of Al₂O₃.

The thermochemical behaviour of the coated powders on continuous heating was studied by DTA up to 1000°C (Fig. 3). The broad endothermic peak at low temperatures is due to elimination of adsorbed H₂O, alcohols and other organic compounds. An exothermic peak evolves at 840 and 905°C for ZT and TZ, respectively. X-ray diffraction (Fig. 4) of samples heated up to 840 and 905°C with the same heating schedule as applied for the DTA runs showed that this exothermic peak results from the crystallization of tetragonal zirconia in the ZrO₂ coatings. In the 905°C samples the diffraction peaks of zirconia are broader in the case of powder TZ compared with powder ZT, indicating a lower grain size of tetragonal zirconia in the former. This can also be observed by TEM: Fig. 5 shows the dark-field image of a small agglomerate of coated particles of sample TZ heated up to 905°C imaged with the

10-1 reflection of Al₂O₃. The ZrO₂ coating consists of tiny zirconia crystallites which give no discrete reflections in the diffraction pattern but only diffraction rings. In contrast, in powder ZT the zirconia diffraction rings are not homogeneous but can be partly resolved into several weak and some strong reflections (220 and 113). Imaging with the 220 reflection of tetragonal zirconia in the dark-field mode reveals some zirconia crystallites that have a size of about 5–20 nm (Fig. 6).

Isothermal heating of the powders at 1200–1550°C for 4 h results in further crystallization of tetragonal zirconia and partial transformation into the monoclinic form. The development of the ratio of tetragonal to monoclinic zirconia was calculated from the X-ray intensities of the (111) diffraction peaks according to Evans *et al.*²⁴ and is represented in Fig. 7. With increasing temperature the tetragonal zirconia content decreases to 53–64% of the total zirconia



(b)

Fig. 2.—Contd.

content at 1300°C. At 1400°C, a sharp increase up to 70–77% tetragonal zirconia was observed which is transformed again at higher temperatures.

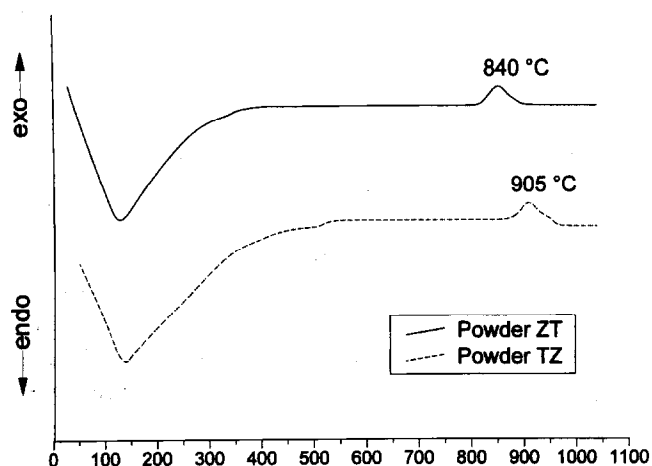


Fig. 3. DTA of the coated powders between 25 and 1040°C, rate of heating 10°C min.⁻¹

At 1300°C the SiO₂ layer reacts with ZrO₂ to give zircon (ZrSiO₄) and cristobalite. At 1400°C the latter has reacted completely with Al₂O₃ to give the first mullite. On prolonged heating at 1400–1550°C zircon reacts with Al₂O₃ to mullite and ZrO₂. Heating the powders at 1550°C for 12 h results in an enhanced growth of ZrO₂ grains. The zircon decomposition and mullite formation is completed and the sample consists only of mullite and tetragonal as well as monoclinic zirconia (Fig. 8). The size of the ZrO₂ crystals seems to be bimodal with one fraction between 1 and 1.5 μm and the other <0.5 μm.

4 Discussion

The present investigation shows that it is possible to coat Al₂O₃ particles with a double layer of SiO₂

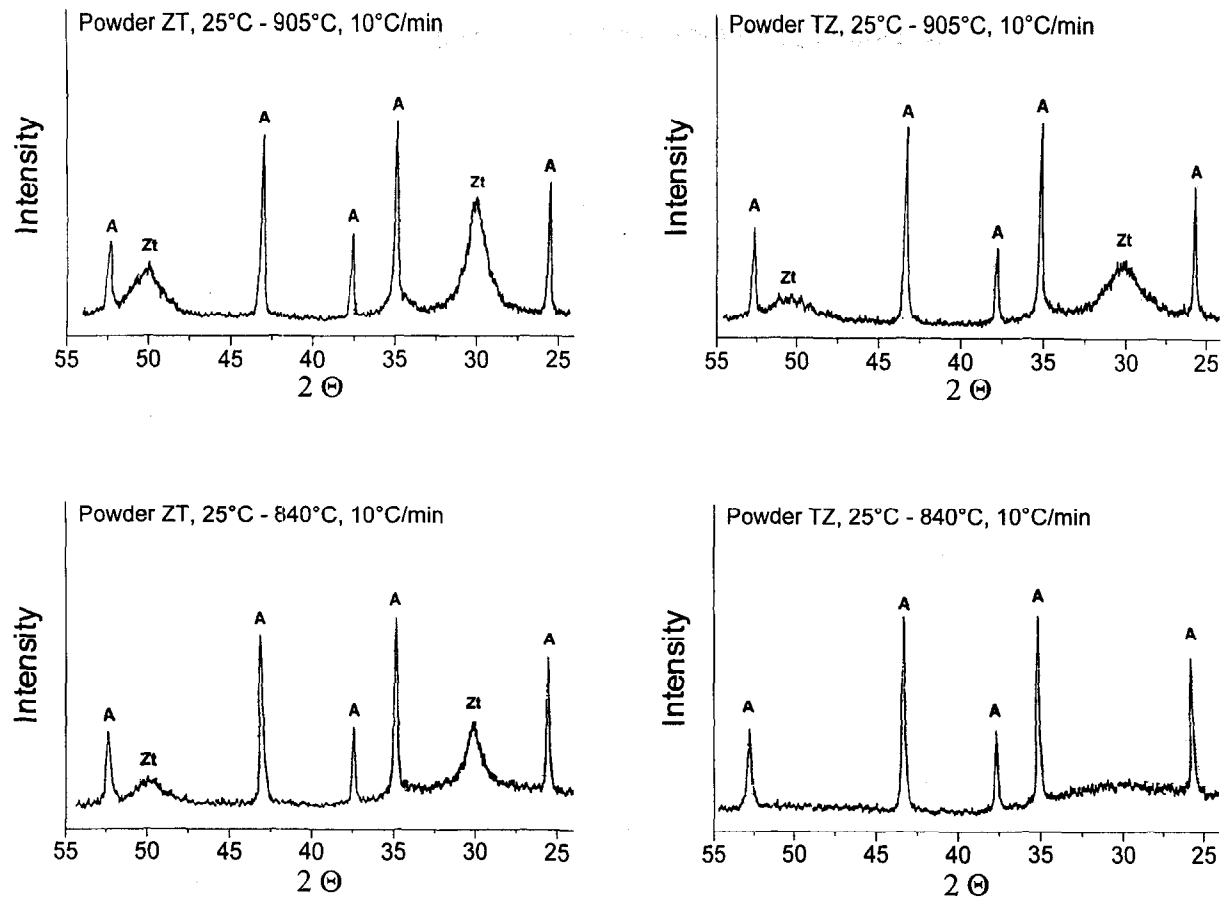


Fig. 4. X-ray diffraction of samples TZ and ZT heated to 840 and 905°C with a heating rate of 10°C min.⁻¹ A indicates the peaks of alumina and Zt those of tetragonal ZrO₂.

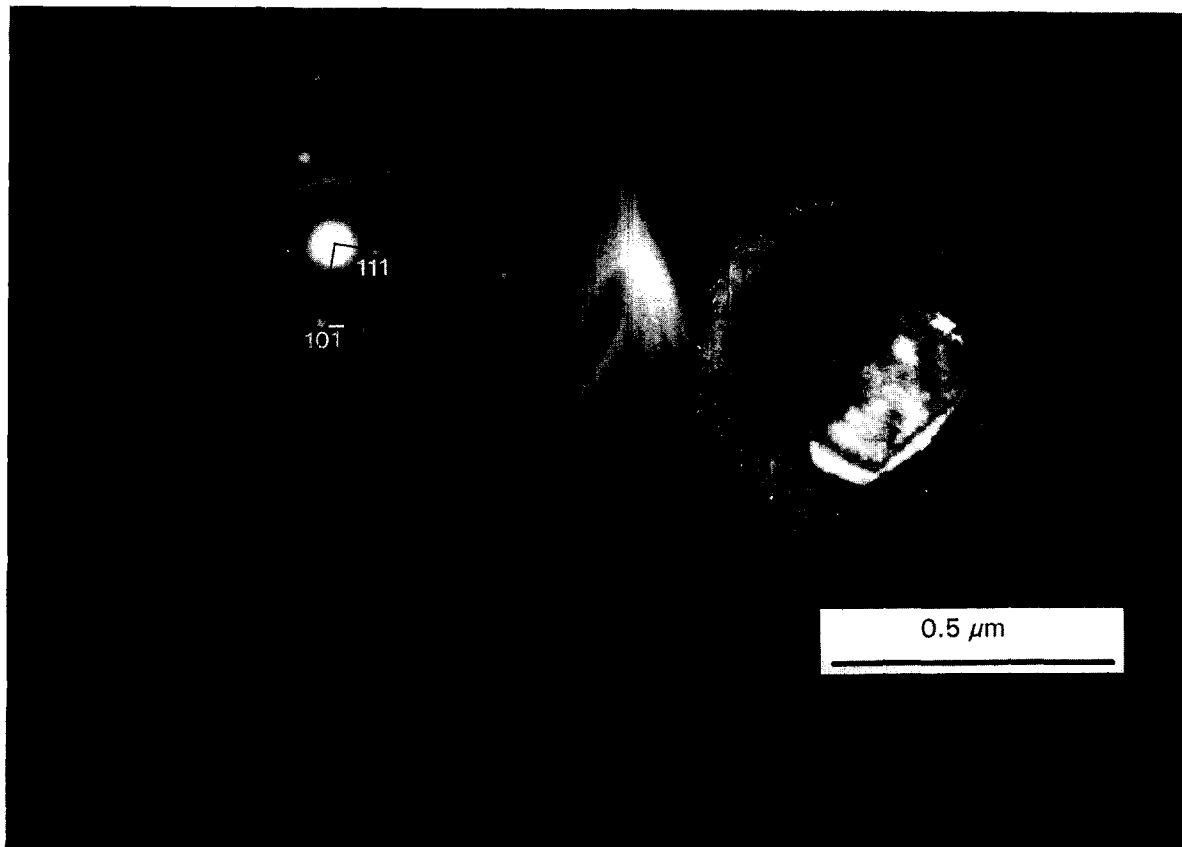


Fig. 5. TEM micrograph of sample TZ continuously heated up to 905°C: (a) Diffraction pattern showing 111 and 10-1 of Al₂O₃ and diffraction rings of tetragonal ZrO₂; (b) dark-field image with 10-1 of Al₂O₃.

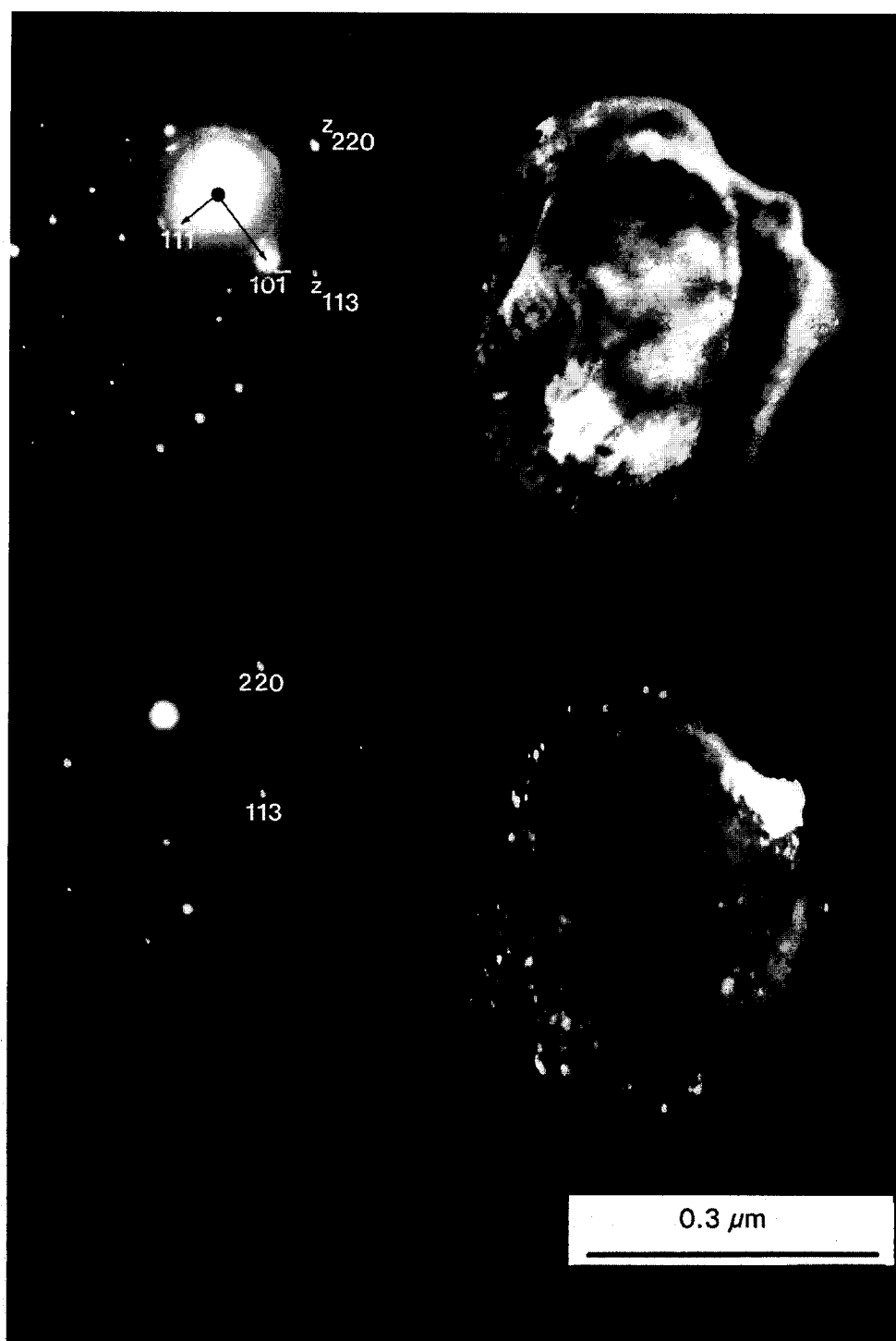


Fig. 6. TEM micrograph of sample ZT continuously heated up to 905°C: (a) diffraction pattern showing 111 and 10-1 of Al₂O₃ and diffraction rings with some discrete reflections (z) of tetragonal ZrO₂; (b) dark-field image with 10-1 of Al₂O₃; (c) dark-field image with 220 of ZrO₂.

and ZrO₂ in a two-step process. The results of DTA measurements indicate the crystallization of tetragonal zirconia at 840 and 905°C, which is in accordance with the results obtained by Palladino *et al.*,²⁵ Nogami *et al.*²⁶ and Ruin *et al.*,¹⁹ who found crystallization temperatures between 800 and 930°C for ZrO₂-SiO₂ gels and ZrO₂-coated alumina powders. The sequence of the SiO₂ and ZrO₂ coatings itself seems to have no great influence on the crystallization and phase reactions

except that the crystallization temperature of sample ZT, where ZrO₂ is the inner coating, is about 65 K lower than that of sample TZ. Obviously, the surface of the crystalline Al₂O₃ core represents a better nucleation site than the surface of the amorphous silicon layer in the case of sample TZ. This is undoubtedly due to a lowering of the heterogeneous nucleation enthalpy by the periodical crystal structure of the alumina surface. Ruin *et al.*,¹⁹ who investigated the coating of Al₂O₃ with

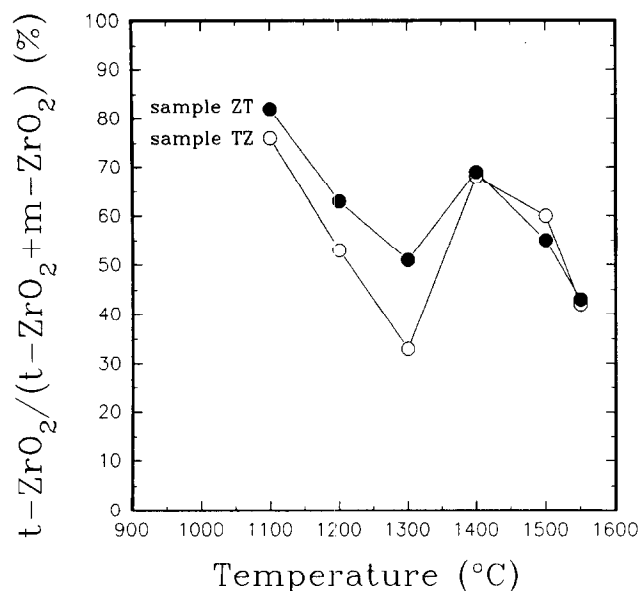


Fig. 7. Development of the tetragonal zirconia content as calculated from X-ray intensities of (111) diffraction peaks of tetragonal and monoclinic zirconia.

ZrO₂, reported an orientation relationship between the tetragonal ZrO₂ crystals and the Al₂O₃ core. In several cases [110] of ZrO₂ was parallel to [11-20] of Al₂O₃. This observation is supported by the similar *d*-values (2.574 and 2.379 Å for tetragonal ZrO₂ and Al₂O₃, respectively) which differ only by 7.5%. Thus, the larger grain size of tetragonal zirconia in sample ZT heated up to 905°C compared with sample TZ is also due to the earlier crystallization and the favourable effect of the Al₂O₃ surface on crystal growth.

Mullite is not formed through the reaction of the SiO₂ layer with the Al₂O₃ core, not even

in sample TZ where SiO₂ and Al₂O₃ are in direct contact. In both samples cristobalite and, in a larger temperature range, zircon appear as precursor phases. Metastable zircon forms above 1200°C but becomes unstable at longer heating times. A remarkable point related to the mullite and zircon formation is the increase of the tetragonal ZrO₂ content at 1400°C. This increase coincides with the beginning of decomposition of zircon, observed from X-ray diffraction. Zircon decomposes into SiO₂ which reacts with Al₂O₃ to form mullite, and ZrO₂ which crystallizes seemingly as tetragonal zirconia. The stability of tetragonal ZrO₂ against transformation into the stable monoclinic polymorph is a function of grain size. ZrO₂ particles in a reaction-sintered mullite matrix smaller than about 1.2 μm keep their tetragonal structure down to room temperature.²⁷ Thus, the ZrO₂ crystals that form from the decomposition products of zircon at 1400°C must be of a relatively small grain size, since a simultaneous increase of the tetragonal zirconia content was observed. Hence, the ZrO₂ crystals observed in samples heated above 1400°C comprise two generations: the first one crystallizes directly from the amorphous ZrO₂ layer and has grown to a size of 1–1.5 μm at 1550°C; the second generation originates from the decomposition of zircon above 1400°C and is of a smaller grain size. This bimodal grain size distribution can be observed by SEM (Fig. 8). In order to maximize the amount of tetragonal zirconia it seems therefore advantageous to favour the metastable formation of zircon and to suppress the direct ZrO₂ crystallization.



Fig. 8. SEM micrograph of sample TZ sintered at 1550°C for 12 h.

References

1. Sparks, R. E., Microencapsulation. In *Encyclopedia of Chemical Technology*, Vol. 15, eds M. Grayson & D. Eckroth. Wiley, New York, 1981, p. 470.
2. Garg, A. & Matijevic, E., Preparation and properties of uniformly coated inorganic colloidal particles. 2. Chromium hydrous oxide on hematite. *Langmuir*, **4** (1988) 38–44.
3. Selmi, F. A. & Amarakoon, V. R. W., Sol-gel coating of powders for processing electronic ceramics. *J. Am. Ceram. Soc.*, **71**[11] (1988) 934–7.
4. Brooks, K. G. & Amarakoon, V. R. W., Sol-gel coating of lithium zinc ferrite powders. *J. Am. Ceram. Soc.*, **74**[4] (1991) 851–3.
5. Fagan, J. G. & Amarakoon, V. R. W., Reliability and reproducibility of ceramic sensors: Part II, PTC thermistors. *Am. Ceram. Soc. Bull.*, **72**[2] (1993) 69–76.
6. Scherer, G. W., Sintering with rigid inclusions. *J. Am. Ceram. Soc.*, **70**[10] (1987) 719–25.
7. Rahaman, M. N. & De Jonghe, L. C., Effect of rigid inclusions on the sintering of glass powder compacts. *J. Am. Ceram. Soc.*, **70**[12] (1987) C348–51.
8. Bordia, R. K. & Scherer, G. W., On constrained sintering — III. Rigid inclusions. *Acta Metall.*, **36**[9] (1988) 2411–16.
9. Scherer, G. W., Viscous sintering of particle-filled composites. *Am. Ceram. Soc. Bull.*, **70**[6] (1991) 1059–63.
10. Hu, C.-L. & Rahaman, M. N., Factors controlling the sintering of ceramic particulate composites: II. Coated inclusion particles. *J. Am. Ceram. Soc.*, **75**[8] (1992) 2066–70.
11. Kim, J. S., Schubert, H. & Petzow, G., Sintering of Si_3N_4 with Y_2O_3 and Al_2O_3 added by coprecipitation. *J. Eur. Ceram. Soc.*, **5** (1989) 311–19.
12. Garg, A. K. & De Jonghe, L. C., Microencapsulation of silicon nitride particles with yttria and yttria-alumina precursors. *J. Mater. Res.*, **5**[1] (1990) 136–42.
13. Kapolnek, D. & De Jonghe, L. C., Particulate composites from coated powders. *J. Eur. Ceram. Soc.*, **7** (1991) 345–51.
14. Wang, C. M. & Riley, F. L., Alumina coating of silicon nitride powder. *J. Eur. Ceram. Soc.*, **10** (1992) 83–93.
15. Kulig, M., Oroschin, W. & Greil, P., Sol-gel coating of silicon nitride with Mg-Al oxide sintering aid. *J. Eur. Ceram. Soc.*, **5** (1989) 209–17.
16. Fegley, B., White, P. & Bowen, H. K., Preparation of zirconia-alumina powders by zirconium alkoxide hydrolysis. *J. Am. Ceram. Soc.*, **68**[2] (1985) C60–2.
17. Guinebretiere, R., Ruin, P., Lecomte, A. & Dager, A., Fabrication and sintering of zirconia sol-gel coated cordierite powder. In *Ceramic Powder Science III Vol. 12*, eds G. L. Messing, S. I. Hirano & H. Hausner. American Ceramic Society, Westerville, OH, 1990, pp. 929–36.
18. Guinebretiere, R., Dager, A. & Lecomte, A., Preparation and densification of zirconia toughened cordierite. In *Eurogel '91*, eds S. Vilminot, R. Nass & H. Schmidt. North-Holland, Amsterdam, 1992, pp. 391–8.
19. Ruin, P., Melin, G., Guinebretiere, R., Lecomte, A. & Dager, A., Coating of oxide powders with alkoxide derived zirconia. *J. Sol-Gel Sci. Technol.*, **2** (1994) 539–44.
20. Sacks, M. D., Bozkurt, N. & Scheiffele, G. W., Fabrication of mullite and mullite-matrix composites by transient viscous sintering of composite powders. *J. Am. Ceram. Soc.*, **74**[10] (1991) 2428–37.
21. Sacks, M. D., Scheiffele, G. W., Bozkurt, N. & Raghu-nathan, R., Fabrication of ceramics and composites by viscous and transient viscous sintering of composite particles. In *Ceramic Powder Science IV Vol. 22*, eds G. L. Messing, S. H. Hirano & H. Hausner, American Ceramic Society, Westerville, OH, 1991, pp. 437–55.
22. Okamura, H., Barringer, E. A. & Bowen, H. K., Preparation and sintering of monosized Al_2O_3 - TiO_2 composite powder. *J. Am. Ceram. Soc.*, **69**[2] (1986) C22–4.
23. Ebener, S., Synthesis of a mullite- ZrO_2 ceramic from sol-gel coated powder. Master thesis, Technical University of Darmstadt, 1994.
24. Evans, P. A., Stevens, R. & Binner, J. G. P., Quantitative X-ray diffraction analysis of polymorphic mixes of pure zirconia. *Br. Ceram. Trans. J.*, **83**[2] (1984) 39–43.
25. Palladino, M., Pirini, F., Chiurlo, P., Cogliati, G. & Costa, L., Sol-gel formation of silica-zirconia glasses. *J. Non-Cryst. Solids*, **147&148** (1992) 335–9.
26. Nogami, M. & Tomozawa, M., Zirconia-transformation-toughened glass-ceramics prepared by the sol-gel process from metal alkoxides. *J. Am. Ceram. Soc.*, **69**[2] (1986) 99–106.
27. Leriche, A., Mechanical properties and microstructures of mullite-zirconia composites. In *Ceramic Trans. Vol. 6: Mullite and Mullite-Matrix Composites*, eds S. Somiya, R. F. Davis & J. A. Pask. American Ceramic Society, Westerville, OH, 1991, pp. 541–51.